RSC Advances

PAPER

View Article Online
View Journal | View Issue

Cite this: *RSC Adv.*, 2015, **5**, 35985

Selective capture of CO_2 by poly(amido amine) dendrimer-loaded organoclays†

Kinjal J. Shah,[a] Toyoko Imae*[ab] and Atindra Shukla[c]

Received 19th March 2015
Accepted 10th April 2015

DOI: 10.1039/c5ra04904k

www.rsc.org/advances

Clay loaded poly(amido amine) dendrimers were explored for capture and storage of CO_2. The loading of dendrimer was promotive in the order of laponite > hydrotalcite > sericite and depended on the surface area of the clays. The CO_2 adsorption on organoclays of laponite and sericite with cationic dendrimer increased with the amount of loaded dendrimer. While CO_2 on pristine laponite was completely released in the desorption process, CO_2 on organo laponite remained in part after the desorption equilibrium. Since the removal of CO_2 from organo laponite was almost comparable to that from pristine clay, it can be mentioned that CO_2 adsorbed on the binding site of laponite is almost desorbed but CO_2 on the binding site of dendrimer is conserved in organoclay. In contrast, in the case of the CO_2 adsorption on the organoclay of hydrotalcite with an anionic dendrimer, the diminution of adsorption sites on hydrotalcite owing to the occupation by dendrimer was observed. It can be mentioned that the cation-exchanged organo laponite loaded amine-terminated dendrimer is a valuable solid adsorbent with a highly selective capture capacity for CO_2.

Introduction

Nowadays, carbon dioxide (CO_2) has become a major environmental issue, because the increasing CO_2 emission is thought to be a main contributor to global warming.[1] Therefore, capture and storage of carbon are a viable strategy for mitigating net CO_2 emission during continuous use of biofuel for energy production.[2] Then, the growing interest of scientists has been focused towards the ways that this gas can be trapped from emission sources, for instance, in an adsorption technique for effective CO_2 capture from the air atmosphere.[3,4] However, there are currently no efficient methods available for separating CO_2 from atmosphere.[5] Over a last few decades, many materials were used for CO_2 adsorption such as porous materials, membranes, solutions, *etc.*[2,6–9] However, the removal of CO_2 through single adsorbent has its limits. In this investigation, the improvement of adsorption capacity of clay using dendrimer was focused, since the clay is very popular adsorbent and dendrimer has capability to encapsulate small molecules.[10,11]

Solid adsorbents have been developed due to their large specific area and specific molecular recognition towards CO_2.[12] The main advantage of solid adsorbents is that the capture of CO_2 occurs, when a CO_2-containing gas is passed through in contact with these solid adsorbents. For industrial application, low-cost solid adsorbents with high capture capacities must be easy produced and regenerated, in spite of difficulties in scaling up of production.[12] In recent years, the adsorption of CO_2 is most investigated on surfaces of oxide,[13] zeolite,[14] silica[15] and clay[16] materials, metal organic frameworks,[17] activated carbons,[18] dendrimers or amine supported materials[16,19] and polymer materials.[7] Especially, layered silicate clays have been proven to be the adequate materials for surface modification by organic molecules such as surfactants and dendrimers[20–22] due to their large surface areas, high ion exchange capacities and unique structural properties such as nanometer-sized platelets with infinitesimal cross-sectional area.[23] Clays provide many active sites, on which the adsorption of inorganic and organic contaminants from aquatic environment is possible.[24]

The adsorption of CO_2 on primary amine is not a new concept in science, since it occurs in nature as exampled by the CO_2 capture of lysine amino acid.[25] Amine-loaded adsorbents have been prepared by two approaches such as surface grafting of aminosilanes and physical adsorption of amine-containing species on adsorbents.[3] Poly(amido amine) (PAMAM) dendrimers are organic molecules characterized by their highly branched three dimensional spherical shapes with a large number of functional terminal groups. For example, fourth-generation (G4) PAMAM dendrimer can load 64 primary amine terminals. Since the number of practical binding sites (nitrogen containing groups) in PAMAM dendrimer increases as increasing the generation of dendrimer, the number of CO_2 molecules to interact with dendrimer should also increase. For

[a]*Graduate Institute of Applied Science and Technology, National Taiwan University of Science and Technology, Taipei 10607, Taiwan. E-mail: imae@mail.ntust.edu.tw*

[b]*Department of Chemical Engineering, National Taiwan University of Science and Technology, Taipei 10607, Taiwan*

[c]*Shah-Schulman Centre for Surface Science and Nanotechnology, Dharmsinh Desai University, Nadiad 387001, India*

† Electronic supplementary information (ESI) available. See DOI: 10.1039/c5ra04904k

capture and separation of CO_2, zeroth generation (G0) PAMAM dendrimer has been immobilized in pores of a polymer membrane.[26] Otherwise, composites of hydroxyl-terminated PAMAM dendrimer and clay are used for adsorbing air pollutants, specially CO_2,[27] but the quantum of adsorption and the elucidation of adsorption sites are a new area for discussion.

The objective of this research is in the development of advanced CO_2-adsorbent materials with effective capture and storage abilities. The developed solid adsorbents are organoclays consisting of PAMAM dendrimer and clay, where amines of a dendrimer in addition to pores of clay are binding sites of CO_2. Cation-exchange clay (laponite and sericite) and anion-exchange clay (hydrotalcite), respectively, were hybridized with G4.0 and G4.5 (amine- and carboxylate-terminated, respectively) PAMAM dendrimers. For the assessment of loading of the dendrimer on the clay, the organoclays were analysed by means of microscopes and methodologies of surface chemistry. Adsorption and desorption studies of CO_2 gas were carried out by the gravimetric method. The behaviours of adsorption and desorption were compared among three systems.

Experimental

Materials

Laponite (XLG) and hydrotalcite clays were purchased from Southern Clay Products Inc. and Wako Chemicals, respectively, and sericite clay (FSN) was donated by Sanshin Mining Ind. Co. Ltd. Concentrated HCl was provided by Fisher Chemicals. Methanol solutions of G4.0 PAMAM dendrimer with amine terminals (molecular weight 14 213) and G4.5 PAMAM dendrimer with sodium carboxylate terminals (molecular weight 26 258) were purchased from Sigma Aldrich. All chemicals above were used without purification.

Instrumentation and techniques

Ultraviolet (UV)-visible absorption spectra were measured using a Jasco V-670 series UV spectrometer with a 1 cm quartz cell. A thermogravimetric analysis (TGA) was carried out at a scan speed of 10 °C min^{-1} under N_2 gas flow on a Q500 TA instrument. Particle size and zeta potential were measured using a Nano Particle Analyser (SZ 100, Horiba). The microscopic observation was performed using a transmission electron microscope (TEM), Hitachi H-7000), equipped with a CCD camera, operating at a voltage of 100 kV. An atomic force microscope (AFM) (Veeco, Digital Instrument Nanoscope III) was operated at the contact mode. The aqueous dispersion of sample powder was dropped on a freshly cleaved mica substrate and dried. The Brunauer–Emmett–Teller (BET) surface area was evaluated from N_2 adsorption–desorption isotherm using a NOVA 1000e surface area analyser. An X-ray diffraction (XRD) analysis was performed on a Bruker D-8 Advance X-ray powder diffractometer having CuKα radiation (=1.5418 Å). The measurement was scanned in 2θ range of 2 to 20 degrees.

Preparation of organoclays

Solvent (methanol) of a PAMAM dendrimer solution were dried by treating with nitrogen gas flow for 1 h at room temperature. Water and clay materials were added to the dendrimers at the stoichiometric weight ratio (0.1–0.7 of dendrimer/clay), where the clay concentration was kept constant. The intercalation process was achieved by adding concentrated HCl drop wise into the suspension to maintain pH (3–7) and by stirring for 2 days at 70 °C in order to attain the intercalation equilibrium as previously reported.[20] After the reacted suspension was centrifuged at 6000 rpm for 5 min, the determination of free dendrimers in the supernatant was performed by measuring the UV-visible absorption spectrum. The residual organoclays were treated several times with washing with water and centrifuging at 6000 rpm for 5 min to remove free dendrimers. The purified organoclays were dried in vacuum for 6 h at 40 °C, following the grind by a pestle in mortar to achieve uniform size. The organoclays prepared by mixing sericite and laponite with G4.0 PAMAM dendrimer and hydrotalcite with G4.5 PAMAM dendrimer at various weight ratios were termed as Ser*n*, Lap*n* and Hyd*n*, where *n* indicates the weight proportion of dendrimer against clay.

Procedures of adsorption and desorption

Adsorption and desorption experiments were carried out on a TGA instrument. The adsorption measurement was carried out at N_2 gas flow (balance chamber) and CO_2 (pure) gas flow (sample chamber) with flow rates of 40 and 60 mL min^{-1}, respectively, at an isotherm condition of 300 min for all organoclays. Temperature dependence for CO_2 and N_2 adsorption was carried out on organoclay (Lap0.7) at different temperatures with the same flow rates of gases and the same measurement time. Clays and organoclays for desorption experiments were prepared first by removing the moisture under N_2 atmosphere and by adsorbing CO_2 for 100 min at room temperature. Then the desorption experiment was performed for 200 min at 40 °C under the flow of N_2 gas.

Results and discussion

Characterization of dendrimer-loaded organoclays

Organoclays were prepared by mixing clays with PAMAM dendrimers at different weight ratios and by treating at acidic condition and high temperature following to the previous report.[20] Cation-exchange laponite and sericite clays were treated with cationic (amine-terminated) G4.0 dendrimer, and anion-exchange hydrotalcite clay was with anionic (carboxylate-terminated) G4.5 dendrimer. Fig. 1 and S1(A)† present UV-visible absorption spectra of supernatants in reaction suspensions, which are attributed to free PAMAM dendrimer non-loaded on cation-exchange (sericite and laponite, respectively) clays. A PAMAM dendrimer solution had an absorption band at 280 nm, and its absorbance changed depending on pH of reaction suspensions. Then the loaded amount of dendrimer on clays can be calculated from such decrease of absorbance. Inset in Fig. 1 and S1(A)† is a plot of dendrimer loading on sericite

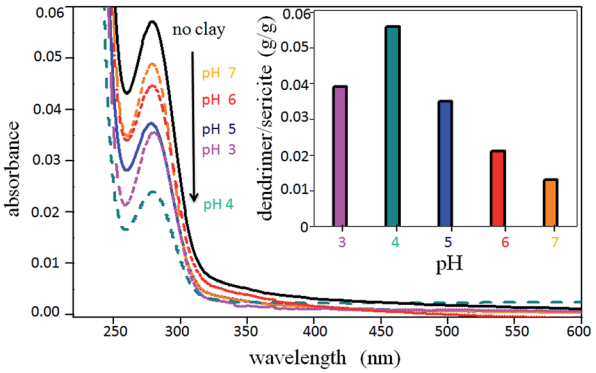

Fig. 1 UV-visible absorption spectra of supernatants after the loading procedure of PAMAM dendrimer (10 mg) on sericite clay (100 mg) at different pH. Solid line with highest absorbance indicates an absorption spectrum of an aqueous dendrimer solution without treatment with clay. Inset is the comparison of dendrimer loading against clay at different pH.

clay at different pH. From this plot, the optimum pH for high loading was found to be pH 4. High loading can be contributed from high protonation of amine in dendrimer at acidic pH[28] and easy cation exchange of sericite and laponite.[29–31] Nevertheless, the decrease of loading at lower pH (<4) is owing to the thinning (or shielding) of electric double layer by condensation of counter ions. High loading was also observed at pH 4 even for the loading of carboxylate-terminated dendrimer on anion-exchange (hydrotalcite) clay (Fig. S1(B)).† The carboxylate-terminated dendrimer is negatively charged at pH > 4.[32] Thus, the preparation of reaction suspensions was carried out at pH 4.

The weight loss experiment in TGA showed that the pristine sericite clay exhibited a weight reduction (5.3%) under heating up to 900 °C in nitrogen atmosphere due to removal of component OH (Fig. 2), although the observed loss was smaller than the calculated content (8.5%) of OH in sericite clay ($KAl_2AlSi_3O_{10}(OH)_2$). In TGA results of organoclays as shown in Fig. 2, the first weight loss occurred around 200–380 °C and the second gradual loss was completed up to 700 °C, where dendrimer and OH component of clay were removed, respectively. Then the loading of PAMAM dendrimer in the clay was calculated as a weight difference between pristine clay and organoclay at 900 °C and found to be in the range of 5.5 to 28.4 wt% for 0.1–0.5 dendrimer/clay weight mixing ratio.

The amounts of PAMAM dendrimers loaded on three clays by exchange of inorganic ions, which were estimated from TGA, are given in Fig. 3. The common feature of dendrimer loading on three clays was that the loading amount was increased initially with dendrimer content and saturated at higher dendrimer content. Saturation happened at dendrimer content in order of sericite < hydrotalcite < laponite, and the saturated loading amount was enlarged in this order (see Table 1). The loading behaviour can be compared with the ion exchange capacity[22,29–31] and the particle size of clay, as seen in Table 1. The increase of dendrimer loading on clay is consistent with the decrease of particle size, but does not necessarily accord with the order of ion exchange capacity. Then the highest loading on laponite can come from smallest platelet size, which causes large specific surface area and a large number of sites for loading.[33]

As seen in Fig. 4(A) and ESI Table S1,† particle sizes of organoclays were increased with increasing of added dendrimer and finally saturated. The increase of particle sizes from pristine clay was nearly three times for laponite and two times for hydrotalcite, while such drastic variation of size could not occur on sericite. Such behaviour can be connected with the amount of dendrimer loading on clay. PAMAM dendrimer adsorbs outer surface of the clay and, at the same time, it can penetrate into interlayer of clay. When dendrimer was intercalated between layers of clay, the interlayer distance of clays can increase about four times, as determined using reflectometry.[34] In addition, dendrimers adsorbed on outer surface may give rise to clay agglomerates, and the agglomeration can easy occur for abundantly dendrimer-adsorbed clays and small-sized clays like laponite. Similar agglomeration by dendrimer has been reported for latex particles.[35]

Since cationic dendrimers should be loaded on cation-exchange clays and *vice versa*, the loading process will effect on overall electrical properties of clays. Zeta potentials of three organoclays were plotted as a function of mixing content of

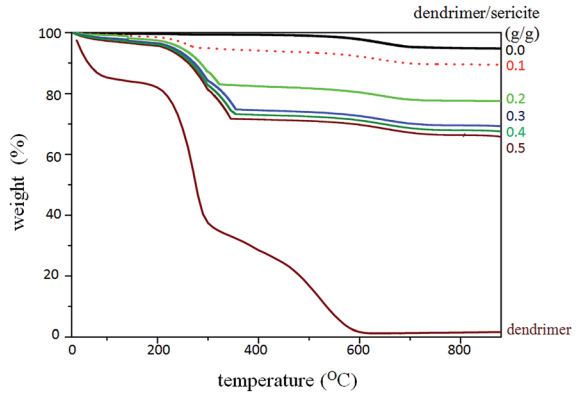

Fig. 2 TGA of PAMAM dendrimer-loaded sericite at different dendrimer/sericite weight mixing ratios in comparison with dendrimer.

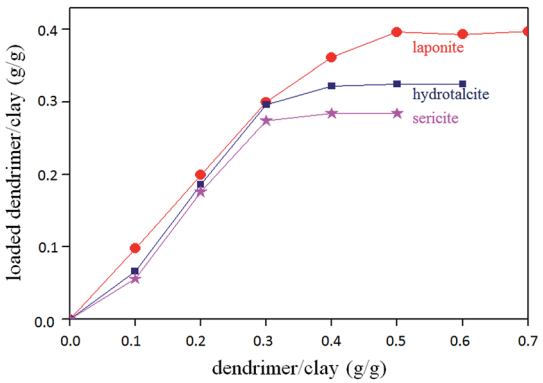

Fig. 3 Dendrimer loading on organoclays as a function of dendrimer/clay weight mixing ratio.

Table 1 Characteristics of pristine and organoclays

Clay/organoclay	Ion exchange capacity (meq g^{-1})	Loading of dendimer per clay (g g^{-1})	Particle size (nm)	Zeta potential (mV)
Lap0.0	0.75 (ref. 27)		42	−111.0
Hyd0.0	3.30 (ref. 26)		130	8.5
Ser0.0	0.25 (ref. 28)		631	−38.5
Lap0.7		0.40	133	140.0
Hyd0.6		0.32	248	−46.5
Ser0.5		0.28	781	8.0

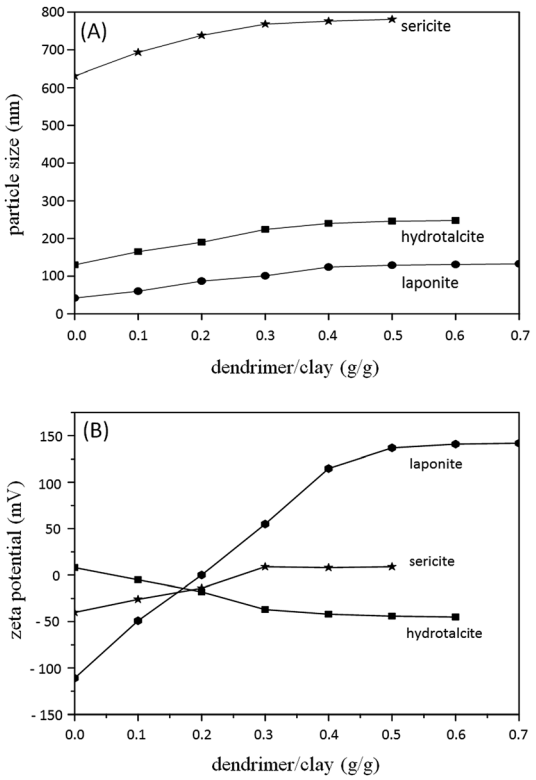

Fig. 4 (A) Particle size and (B) zeta potential of pristine and organoclays as a function of dendrimer/clay weight mixing ratio.

dendrimer in Fig. 4(B). On cation-exchange clays of laponite and sericite, zeta potentials varied from negative to positive with an increased amount of positively charged amine-terminated dendrimer, while on anion-exchange hydrotalcite clay, zeta potentials changed from positive to negative, as a dendrimer has a negatively charged carboxyl terminals. Then, as well as the behavior of particle size, the zeta potential values were saturated at high dendrimer contents, where the saturation happened just at the same concentration with the saturation of dendrimer loading. This indicates that the behavior of zeta potential variation is related to that of the amount of dendrimer loaded on the clay. As seen in Table 1, the saturated zeta potential of laponite were higher than that of sericite, and this tendency is consistent with that of dendrimer loading on clay as seen in Fig. 3. When the variation of the zeta potential from pristine clay to loading-saturated clay was calculated (see Table 1), the tendency of the variation was qualitatively consistent with the dendrimer loading, although the variation was not quantitatively in proportion with the loading amount of the dendrimer and the variation on laponite was larger than other clays. This result indicates that the zeta potential reflects any factor besides the loading of dendrimer.

The BET surface areas and pore sizes of pristine clays and organoclays at the saturated loading amounts of dendrimers on clays are listed in Table 2. Laponite had a significantly large BET surface area compared to hydrotalcite and sericite due to its small platelet size. Furthermore, it can be seen that the available BET surface area decreased remarkably on laponite and moderately on hydrotalcite and sericite, after PAMAM dendrimer was loaded, in consistency with the high loading of dendrimer on laponite because of the large surface area of laponite. The pore size of organoclays increased 3, 1.5 and 1.1 times larger than pristine clays in the case of laponite, hydrotalcite and sericite respectively, depending on significant loading of modifier, namely, PAMAM dendrimer, in the clay pores. Table 2 compares *d*-spacing from XRD between pristine clays and organoclays. Since the inorganic ions inside the interlayer space of clay were replaced by PAMAM dendrimers, the layer repeating distance (*d*-spacing, about 1 nm) of pristine clays increased commonly about 1 nm for all organoclays. This is reasonable, since dendrimers can be intercalated in the interlayer of clay by planularly distorting and as a monomolecular layer,[20] independent of clay species. Maximum *d*-distance of 21 nm is rather thinner than the size of dendrimer in solution.[36] Shape change of dendrimer to become "pancake" can happen in the organoclays because of flexible configuration of dendrimer.[34,37] Similar shape change of dendrimer has been reported on substrate and between bilayers.[38,39]

To investigate the morphologies of pristine clay and organoclay, TEM and AFM observations were performed. Fig. 5

Table 2 BET surface area, average pore size and *d*-spacing of pristine and organoclays

Clay	BET surface area (m^2 g^{-1})	Average pore size (Å)	*d*-spacing (Å)
Lap0.0	358	27.5	9.9
Hyd0.0	59	142.0	9.8
Ser0.0	12	103.0	10.0
Lap0.7	107	78.3	21.4
Hyd0.6	41	213.1	17.3
Ser0.5	9	114.9	20.8

shows TEM photographs of pristine (Ser0.0) and organoclay (Ser0.1) of sericite. Organoclay of sericite was still keeping a flat sheet texture even after the dendrimer was adsorbed on clay (see Fig. 5(B)). Whereas, while the pristine clay displayed the smooth surface and edge (Fig. 5(C)), the organoclay showed the presence of many small spots on the surface and edge, as compared with Fig. 5(D). Since the size of spots is around 4 nm, these spots can be assigned to be PAMAM dendrimers.

AFM images of pristine sericite (Ser0.0) and its organoclay (Ser0.5) are shown in Fig. 6. The images (Fig. 6(A) and (B)) indicated the accumulation of clay plates. While the surface analysis (Fig. 6(C)) on clay revealed the flatness of the clay surface (roughness: 0.6 nm), the AFM image of the organoclay pointed out the surface with about 3–4 nm roughness as shown in Fig. 6(D). This texture gives a confirmation of PAMAM dendrimer on the clay. The existence of the dendrimer on the clay observed by TEM and AFM was also confirmed by the zeta potential and BET results, as described already.

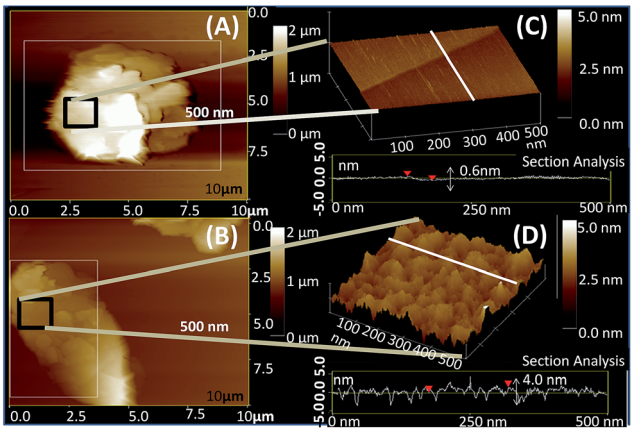

Fig. 6 AFM Images of (A and C) pristine (Ser0.0) and (B and D) organo sericite (Ser0.5).

CO_2 adsorption and desorption

The ideal solid material as a candidate for CO_2 capture should possess effective CO_2 selectivity, high adsorption capacity and easy regeneration. Then, the following factors must be taken into account for selecting the adsorbents; that is, the efficiency and temperature of reaction. The CO_2 adsorption of pristine clay and organoclays with different loading amount of PAMAM dendrimer, which was measured at room temperature under CO_2 atmosphere, is shown in Fig. S2.† In common, the CO_2 adsorption started after exposed the clay or organoclay to CO_2 gas and then reached saturation at any reaction time, although some systems did not reach the saturation even after 300 min reaction. The amounts of CO_2 adsorption at 300 min reaction for three clays are plotted in Fig. 7 as a function of mixing ratio of dendrimer and clay. Pristine clays had their individual CO_2 adsorption capacities. Among them, laponite (cation-exchange clay) had the highest CO_2 adsorption capacity, and hydrotalcite (anion-exchange clay) had a higher CO_2 absorption capacity than sericite (cation-exchange clay). This suggests that CO_2 adsorption is not affected by only charge of clays, but other factors like surface area also influence on the adsorption properties. As shown in Table 2, pristine clays have BET surface areas in the order of laponite > hydrotalcite > sericite. It should be noted that clay with high surface area possesses high probability of CO_2 adsorption.

After the loading of PAMAM dendrimer on clay, two types of behaviours depending on clays were observed during the CO_2 adsorption as shown in Fig. 7. For both cation-exchange clays (laponite and sericite), adsorption amounts of CO_2 were increased with loading cationic dendrimer. Since the BET surface areas of organoclays were lower than pristine clays (see Table 2), the pristine clay with high surface area may exhibit high CO_2 adsorption from a commonsense. However, Fig. 7 revealed that CO_2 adsorption was higher on organoclays than on their pristine laponite and sericite. These results suggest the possibility of CO_2 adsorption on dendrimer loaded on clays beside the adsorption on clay surface. As the loading of PAMAM dendrimer increases, CO_2 adsorption on laponite and sericite

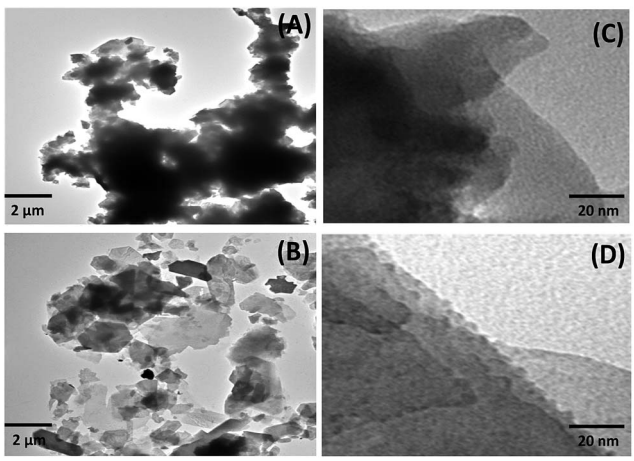

Fig. 5 TEM Images of (A and C) pristine (Ser0.0) and (B and D) organo sericite (Ser0.1).

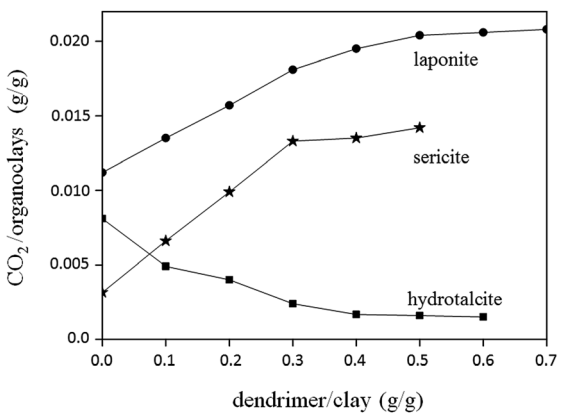

Fig. 7 CO_2 adsorption on pristine and organoclays as a function of dendrimer/clay weight mixing ratio.

clays increased in parallel each other. This behaviour can be compared with the dendrimer loading on clays (see Fig. 3).

Meanwhile, for anion-exchange hydrotalcite clay, the CO_2 adsorption was contrary decreased with increasing dendrimer content, different from cases of laponite and sericite. In this case, G4.5 PAMAM dendrimer terminated by carboxyl group may not adsorb CO_2 because of no affinity between them. Although the pristine hydrotalcite can adsorb CO_2 due to enough large BET surface area, the capacity of CO_2 adsorption on clay is diminished by the occupation of clay surface by dendrimer and, therefore, CO_2 adsorption on organoclay goes down from the adsorption on pristine clay. When the proportion of dendrimer to clay was increased, CO_2 adsorption was almost saturated above Lap0.5, and similar saturation happened at Ser0.3 and Hyd0.4. These proportions of dendrimer for saturation of CO_2 adsorption are consistent with the proportions for saturation of dendrimer loading on clays, particle size and zeta potential of organoclays. This consistency suggests that CO_2 adsorption is involved in these factors.

Temperature is one of the important parameters on CO_2 adsorption. The experiment by means of the TGA showed that both CO_2 and N_2 adsorptions decreased with an increase in temperature as shown in Fig. S3,† which plots the adsorption of CO_2 and N_2 on Lap0.7 up to 300 min at various temperatures. Then the adsorption amounts of CO_2 and N_2 at 300 min were plotted in Fig. 8(A) as a function of temperature. Fig. 8(A) indicates that the adsorption of N_2 gas at temperature below 150 °C was almost negligible compared to CO_2 gas, suggesting no efficient affinity of this organoclay with N_2 gas. Meanwhile, the amount of CO_2 adsorption decreased from 0.02 g g^{-1} clay at 30 °C to almost zero at 150 °C. The same trend of decreasing adsorption of both CO_2 and N_2 gases was also seen at temperatures from 150 to 190 °C, but during this temperature raise, the corresponding weight underwent a negative change, which suggests the weight loss of organoclay.

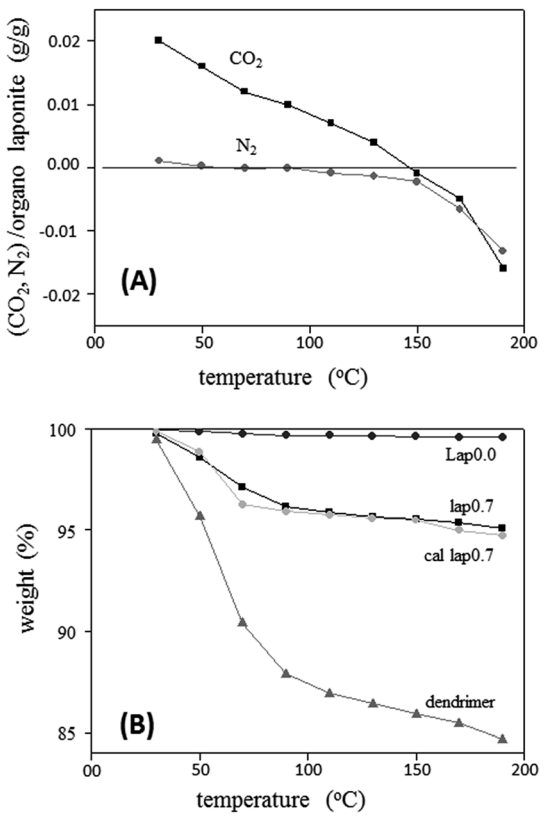

Fig. 8 (A) Temperature dependence of CO_2 and N_2 adsorption on organo laponite (Lap0.7). (B) TGA of pristine (Lap0.0), organo laponite (Lap0.7) and PAMAM dendrimer in comparison with calculated organo laponite (Lap0.7).

In order to interpret the temperature dependence of CO_2 adsorption, TGA of pristine laponite (Lap0.0), laponite organoclay (Lap0.7) and dendrimer were measured. It could be seen from Fig. 8(B) that while the component weight loss of clay along with temperature rise was very less, the weight loss of organoclay increased with temperature and the profile of weight loss was consistent with the calculation, which was carried out based on the 0.7 mixing proportion from data of Lap0.0 and dendrimer. The weight loss of dendrimer at temperature below 190 °C is known to be due to the removal of volatile chemicals such as water and methanol, but not the decomposition of dendrimer.[40] Thus, the temperature-depending apparent decrease of CO_2 adsorption is underestimated because of the removal of volatile chemicals from dendrimer: the removal of volatile chemicals overcomes the CO_2 adsorption at temperature above 150 °C, and then the apparent CO_2 adsorption becomes negative.

From the viewpoint of practical application, the adsorption on adsorbents should be specified for their components, for instance for clay and dendrimer in organoclay. Then desorption experiments were performed on pristine and organoclays of laponite to determine the desorption ability of adsorbents. The representative data are shown in Fig. 9(A), which plots the adsorption (100 min) and desorption (200 min) processes of CO_2 gas on Lap0.0 and Lap0.5 clays at 40 °C. The adsorption and desorption processes happened exponentially with time and approached to saturation of adsorption and desorption, respectively. Then adsorbed ((a), at 100 min), desorbed ((d), at 300 min) and remained (a–d) amounts of CO_2 on clays were plotted in Fig. 9(B) as a function of mixing proportion of dendrimer. It can be seen that the adsorbed CO_2 molecules were desorbed 100% for the pristine clay, but they on the organoclay remained. The remaining CO_2 molecules were almost comparable to the increased amount with increasing proportion of dendrimer. This suggests that CO_2 molecules adsorbed on clay surface are almost released, but CO_2 molecules captured by dendrimer remain in organoclays.

Based on the results obtained in this investigation, the aspect of adsorption and desorption of CO_2 on pristine clay and organoclay of laponite is presented in Scheme 1. In case of the addition of dendrimer having cationic terminal groups, the adsorption of the dendrimer is governed by ionic exchange of small inorganic ions on cation-exchange laponite clay and attracted by electrostatic interaction on the clay. The exchange occurs on the clay surface and in the interlayer of clay sheets. On the latter case, *d*-spacing of sheets is expanded, as observed by XRD.

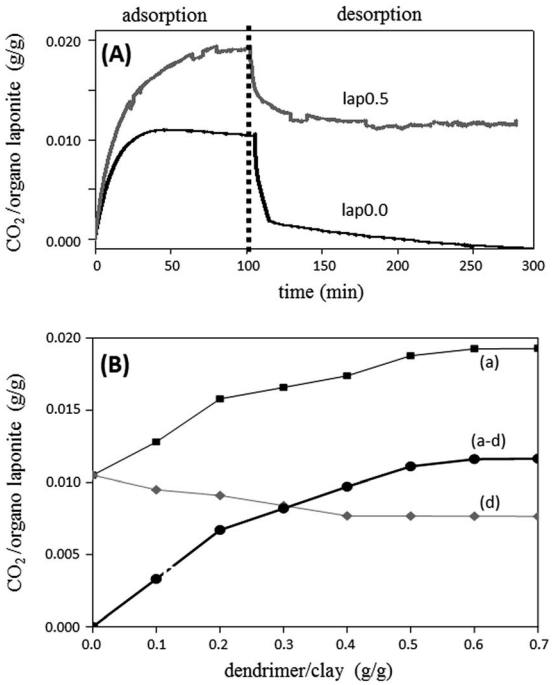

Fig. 9 (A) CO_2 adsorption/desorption on pristine (lap0.0) and organo laponite (lap0.5). (B) CO_2 contents on pristine and organo laponite as a function of dendrimer/laponite weight mixing ratio. (a) Adsorbed, (d) desorbed and (a–d) remained.

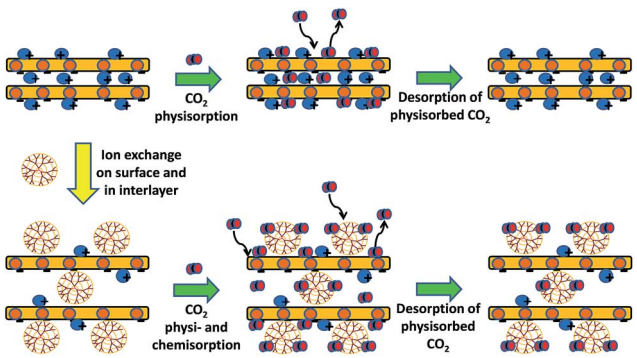

Scheme 1 Estimated process of dendrimer loading and CO_2 adsorption/desorption on laponite.

Although pristine laponite does not have any reactive sites for CO_2 gas molecules, some gas molecules are adsorbed on clay surface and in interlayer of clay due to the existing adsorption pores in the clay. This phenomenon can be called as physisorption of CO_2 gas molecules on clay moiety. In case of laponite organoclays, the adsorption capacity of CO_2 gas is higher than that of pristine clay, because organoclays have additional adsorption site beside pores on clay to capture CO_2. The additional site must be on dendrimer moieties in organoclays; maybe, amines of dendrimer.

During the desorption process of pristine laponite, CO_2 gas molecules remove mostly from clay, since CO_2 molecules very loosely bond, maybe, by van der Waals attraction on pristine clay. On the other hand, on the desorption process of organoclays, CO_2 adsorbed on clay moiety of organoclays can easy remove as well as on the pristine clay. However, remaining CO_2 molecules bind too tightly on dendrimer moiety to remove. This suggests that the adsorption on dendrimer moiety has high affinity towards CO_2 gas for adsorbing tightly.

Conclusions

In this work, low cost and commercially available nanoclays have been used to develop dendrimer-loaded solid adsorbents for CO_2 adsorption. The high loading of dendrimer on the adsorbents depends on the size and binding site of clay materials, as confirmed by a series of characterization experiments like TEM, AFM and particle analyser. Laponite clay, which has high ion exchange capacity, provides more favourable cation-exchange sites for cationic PAMAM dendrimer than sericite with low ion exchange capacity. For anion-exchange hydrotalcite clay, anionic dendrimer is adequate to reach enough loading of dendrimer.

The capability of CO_2 gas adsorption on pristine clays is the same order as the dendrimer loading, that is, laponite > hydrotalcite > sericite. However, the behaviour of CO_2 adsorption on organoclays does not follow this order. Cation-exchange clays (laponite and sericite) behave similar each other. They have at least two binding sites of clay and dendrimer moieties in organoclays. While CO_2 molecules adsorbed on pristine clays are desorbed mostly, CO_2 adsorption on organoclays increases with increasing the loading of dendrimer, but some CO_2 molecules on organoclays remain after desorption procedure. This indicates that CO_2 molecules adsorbed on binding sites of dendrimer are not easy desorbed. Meanwhile, CO_2 adsorption on organo hydrotalcite rather decreases with increasing dendrimer content. This mentions that carboxylate terminals on dendrimer adsorbed on hydrotalcite keep off CO_2 molecules from the adsorption on dendrimer and clay. This indicates that organoclays consisting of dendrimers with different types of terminal groups (amine or carboxylate) are differently responsible for CO_2 capture.

Thus, this study shows that solid adsorbents with a highly selective capture capacity can be made from low cost nanoclays, which work over a wide range of capture conditions.

Acknowledgements

This work was financially supported by National Taiwan University of Science and Technology, Taiwan, under grant number 100H451201. KS appreciates the financial support from National Taiwan University of Science and Technology, Taiwan, for student scholarship. The authors gratefully thank Prof. M. Ujihara, National Taiwan University of Science and Technology, Taiwan, for his technical support.

References

1 R. Dawson, E. Stöckel, J. R. Holst, D. J. Adams and A. I. Cooper, *Energy Environ. Sci.*, 2011, **4**, 4239–4245.

2 H. Yang, Z. Xu, M. Fan, R. Gupta, R. B. Slimane, A. E. Bland and I. Wright, *J. Environ. Sci.*, 2008, **20**, 14–27.
3 A. Heydari-Gorji and A. Sayari, *Chem. Eng. J.*, 2011, **173**, 72–79.
4 J. Kim, L. C. Lin, J. A. Swisher, M. Haranczyk and B. Smit, *J. Am. Chem. Soc.*, 2012, **134**, 18940–18943.
5 A. Zhao, A. Samanta, P. Sarkar and R. Gupta, *Ind. Eng. Chem. Res.*, 2013, **52**, 6480–6491.
6 S. Kentish, C. Scholes and G. Stevens, *Recent Pat. Chem. Eng.*, 2008, **1**, 52–66.
7 H. A. Patel, F. Karadas, A. Canlier, J. Park, E. Deniz, Y. Jung, M. Atilhan and C. T. Yavuz, *J. Mater. Chem.*, 2012, **22**, 8431–8437.
8 H. A. Patel and C. T. Yavuz, *Chem. Commun.*, 2012, **48**, 9989–9991.
9 R. Dawson, L. A. Stevens, T. C. Drage, C. E. Snape, M. W. Smith, D. J. Adams and A. I. Cooper, *J. Am. Chem. Soc.*, 2012, **134**, 10741–10744.
10 D. Kannaiyan and T. Imae, *Langmuir*, 2009, **25**, 5282–5285.
11 G. Saravanan and T. Imae, *J. Nanosci. Nanotechnol.*, 2011, **11**, 4838–4845.
12 E. A. Roth, S. Agarwal and R. K. Gupta, *Energy Fuels*, 2013, **27**, 4129–4136.
13 R. Serna-Guerrero, E. Da'na and A. Sayari, *Ind. Eng. Chem. Res.*, 2008, **47**, 9406–9412.
14 M. R. Hudson, W. L. Queen, J. a. Mason, D. W. Fickel, R. F. Lobo and C. M. Brown, *J. Am. Chem. Soc.*, 2012, **134**, 1970–1973.
15 B. Fadhel, M. Hearn and A. Chaffee, *Microporous Mesoporous Mater.*, 2009, **123**, 140–149.
16 W. Wang, X. Wang, C. Song, X. Wei, J. Ding and J. Xiao, *Energy Fuels*, 2013, **27**, 1538–1546.
17 K. Sumida, D. L. Rogow, J. a. Mason, T. M. McDonald, E. D. Bloch, Z. R. Herm, T.-H. Bae and J. R. Long, *Chem. Rev.*, 2012, **112**, 724–781.
18 R. V. Siriwardane, M. Shen, E. P. Fisher and J. A. Poston, *Energy Fuels*, 2001, **15**, 279–284.
19 A. C. C. Chang, S. S. C. Chuang, M. Gray and Y. Soong, *Energy Fuels*, 2003, **17**, 468–473.
20 A. S. Costa, T. Imae, K. Takagi and K. Kikuta, *Prog. Colloid Polym. Sci.*, 2004, **128**, 113–119.
21 A. S. Costa and T. Imae, *Langmuir*, 2004, **20**, 8865–8869.
22 K. J. Shah, M. K. Mishra, A. D. Shukla, T. Imae and D. O. Shah, *J. Colloid Interface Sci.*, 2013, **407**, 493–499.
23 S. M. Lee and D. Tiwari, *Appl. Clay Sci.*, 2012, **59–60**, 84–102.
24 L. B. de Paiva, A. R. Morales and F. R. Valenzuela Díaz, *Appl. Clay Sci.*, 2008, **42**, 8–24.
25 X. Wang, N. G. Akhmedov, Y. Duan, D. Luebke, D. Hopkinson and B. Li, *ACS Appl. Mater. Interfaces*, 2013, **5**, 8670–8677.
26 A. S. Kovvali and K. K. Sirkar, *Ind. Eng. Chem. Res.*, 2001, **40**, 2502–2511.
27 A. Azzouz, E. Assaad, A.-V. Ursu, T. Sajin, D. Nistor and R. Roy, *Appl. Clay Sci.*, 2010, **48**, 133–137.
28 D. Leisner and T. Imae, *J. Phys. Chem. B*, 2003, **107**, 13158–13167.
29 A. Vaccari, *Catal. Today*, 1998, **41**, 53–71.
30 N. Negrete-Herrera, J.-L. Putaux and E. Bourgeat-Lami, *Prog. Solid State Chem.*, 2006, **34**, 121–137.
31 Y. Shih and Y. Shen, *Appl. Clay Sci.*, 2009, **43**, 282–288.
32 R. C. van Duijvenbode, G. J. M. Koper and M. R. Bohmer, *Langmuir*, 2000, **16**, 7713–7719.
33 N. N. Herrera, J. Letoffe, J. Putaux, L. David and E. Bourgeat-lami, *Langmuir*, 2004, **20–5**, 1564–1571.
34 K. Mitamura and T. Imae, *Trans. Mater. Res. Soc. Jpn.*, 2003, **28**, 71–74.
35 W. Lin, P. Galletto and M. Borkovec, *Langmuir*, 2004, **20**, 7465–7473.
36 M. F. Ottaviani, P. Andechaga, N. J. Turro and D. A. Tomalia, *J. Phys. Chem. B*, 1997, **101**, 6057–6065.
37 A. S. Costa and T. Imae, *Trans. Mater. Res. Soc. Jpn.*, 2004, **29**, 3211–3214.
38 X. Li, T. Imae, D. Leisner and M. A. López-Quintela, *J. Phys. Chem. B*, 2002, **106**, 12170–12177.
39 M. Ito and T. Imae, *J. Nanosci. Nanotechnol.*, 2006, **6**, 1667–1672.
40 O. Ozturk, T. J. Black, K. Perrine, K. Pizzolato, C. T. Williams, F. W. Parsons, J. S. Ratliff, J. Gao, C. J. Murphy, H. Xie, H. J. Ploehn and D. a. Chen, *Langmuir*, 2005, **21**, 3998–4006.